Palestine Journal of Mathematics

Vol. 5(Special Issue: 1) (2016) , 228–237

THIRD ORDER NON-OSCILLATORY CENTRAL SCHEME FOR MULTIDIMENSIONAL HYPERBOLIC CONSERVATION LAWS

A. A. I. Peer, A. A. E. F. Saib, M. S. Sunhaloo and M. Bhuruth

Communicated by Suheil Khoury

MSC 2010 Classifications: Primary 65M08; Secondary 35L65.

Keywords and phrases: Multidimensional hyperbolic conservation laws, non-oscillatory central scheme, non-linear limiters.

Abstract. We derive a third-order non-oscillatory central scheme for multidimensional hyperbolic systems. We use computationally efficient limiters in order to make the new scheme non-oscillatory. The solution is advanced in time using natural continuous extension of Runge-Kutta methods. We pay particular attention to two dimensional problems including inviscid Burgers' equation and Riemann gas dynamics problems. Numerical experiments show that the new scheme remains non-oscillatory while giving good resolution of discontinuities.

1 Introduction

Multidimensional hyperbolic conservation laws of the form

$$u_t + \nabla_{\mathbf{x}} \cdot f(u) = 0, \quad \mathbf{x} \in \mathbb{R}^d, \tag{1.1}$$

and with initial data $u(\mathbf{x},\, t = 0) = u_0(\mathbf{x})$, have been used as models for a wide variety of physical phenomena. Examples include the Buckley-Leverett equation for modelling a one-dimensional two-phase flow of immiscible fluids through porous media [3] and the Euler equations of gas-dynamics [25, 14]. Other examples can be found in the book by [7].

Some major developments in central schemes for multidimensional problems include non-oscillatory piecewise polynomial reconstructions by [5, 6]. A class of multidimensional central weighted essentially non-oscillatory (CWENO) methods was developed in [16, 15, 17]. These schemes enjoy a black-box approach, that is, only the flux is required and can be extended to most hyperbolic problems, e.g. [18]. A family of semi-discrete central schemes for solving multidimensional problems has been proposed in [8, 11, 10, 9], which are advanced in time with ODE solvers.

In this work, we develop a third order non-oscillatory central scheme for approximating multidimensional hyperbolic conservation laws (1.1). The new scheme is genuinely non-oscillatory in the sense of [20, 21] compared to ENO reconstructions. It combines the minmod limiter with a quadratic polynomial. Though, the scheme can be applied as a black-box solver, we will be paying special attention to the numerical solution of multidimensional inviscid Burgers' equation and Euler equations of gas dynamics.

The outline of this paper is as follows: In Sect. 2, the general approach for solving multidimensional problems using staggered central schemes is presented. The reconstruction of our new scheme is discussed in Sect. 3. In Sect. 4 some numerical examples are given and solved with the proposed method. The paper ends with conclusion in Sect. 5.

2 Multi-Dimensional Central Schemes

For simplicity, we consider the two-dimensional problem, where $d = 2$ in (1.1)

$$u_t + f(u)_x + g(u)_y = 0. \tag{2.1}$$

We further consider a uniformly discretised cell-centered computational domain where $I_{ij} = [x_{i-\frac{1}{2}}, x_{i+\frac{1}{2}}] \times [y_{j-\frac{1}{2}}, y_{j+\frac{1}{2}}]$ and the width in the x and y directions are respectively denoted by h and k. For simplicity, we describe the case when $h = k$. The cell-centres are given by (x_i, y_j) where $x_i = \frac{1}{2}(x_{i-\frac{1}{2}} + x_{i+\frac{1}{2}})$ and $y_j = \frac{1}{2}(y_{j-\frac{1}{2}} + y_{j+\frac{1}{2}})$.

In central schemes, the cell-averages at time t^n given by

$$\overline{u}^n_{ij} = \frac{1}{h^2} \int \int_{I_{ij}} u(x, y, t^n)\, dy\, dx,$$

are assumed to be known. Then a piecewise polynomial interpolating the cell averages is used

$$u^n(x, y) = \sum_{i,j} p^n_{i,j}(x, y)\, \chi_{i,j}(x, y), \tag{2.2}$$

where $\chi_{ij}(x, y)$ is the characteristic function of the cell I_{ij}.

Integrating (2.1) over $I_{i+\frac{1}{2},j+\frac{1}{2}} \times [t^n, t^{n+1}]$, gives the fully discrete scheme

$$\begin{aligned}
\overline{u}^{n+1}_{i+\frac{1}{2},j+\frac{1}{2}} =& \overline{u}^n_{i+\frac{1}{2},j+\frac{1}{2}} \\
&- \frac{1}{h^2} \left\{ \int_{\tau=t^n}^{t^{n+1}} \int_{y=y_j}^{y_{j+1}} [f\,(u(x_{i+1}, y, \tau)) - f\,(u(x_i, y, \tau))] dy\, d\tau \right\} \\
&- \frac{1}{h^2} \left\{ \int_{\tau=t^n}^{t^{n+1}} \int_{x=x_i}^{x_{i+1}} [g\,(u(x, y_{j+1}, \tau)) - g\,(u(x, y_j, \tau))] dx\, d\tau \right\},
\end{aligned} \tag{2.3}$$

where the staggered cell average $\overline{u}^n_{i+\frac{1}{2},j+\frac{1}{2}}$ are obtained from (2.2) as follows:

$$\begin{aligned}
\overline{u}^n_{i+\frac{1}{2},j+\frac{1}{2}} =& \frac{1}{h^2} \int \int_{I_{i+\frac{1}{2},j+\frac{1}{2}}} u^n(x, y) dy\, dx \\
=& \frac{1}{h^2} \left[\int_{x_i}^{x_{i+\frac{1}{2}}} \int_{y_j}^{y_{j+\frac{1}{2}}} p^n_{i,j}(x, y)\, dy\, dx + \int_{x_i}^{x_{i+\frac{1}{2}}} \int_{y_{j+\frac{1}{2}}}^{y_{j+1}} p^n_{i,j+1}(x, y)\, dy\, dx \right. \\
&\left. + \int_{x_{i+\frac{1}{2}}}^{x_{i+1}} \int_{y_j}^{y_{j+\frac{1}{2}}} p^n_{i+1,j}(x, y)\, dy\, dx + \int_{x_{i+\frac{1}{2}}}^{x_{i+1}} \int_{y_{j+\frac{1}{2}}}^{y_{j+1}} p^n_{i+1,j+1}(x, y)\, dy\, dx \right].
\end{aligned} \tag{2.4}$$

The integrals of (2.3) are evaluated by reconstructing the point values of $\{u(x, y, \tau) | t^n \le \tau \le t^{n+1}\}$ from the known cell-averages. Then, for a sufficiently small time step Δt, the integrals are assumed to be smooth, such that appropriate quadrature rules can be used. For example, one can use the following quadrature rule in space:

$$\int_{x_i}^{x_{i+1}} f(x) dx = \frac{h}{24} \left[-f(x_{i+2}) + 13 f(x_{i+1}) + 13 f(x_i) - f(x_{i-1}) \right] + \mathcal{O}(h^4), \tag{2.5}$$

and the Simpson's rule given by:

$$\int_{\tau=t^n}^{t^{n+1}} f\,(u(x_i, y_j, \tau))\, d\tau = \Delta t \sum_{l=0}^{m} \gamma_l \left[f\,(u(x_i, y_j, t^n + \beta_l \Delta t)) \right], \tag{2.6}$$

to evaluate the time integrals where $\beta_0 = 0$, $\beta_1 = 1/2$, $\beta_2 = 1$, $\gamma_0 = 1/6$, $\gamma_1 = 2/3$ and $\gamma_2 = 1/6$. For this quadrature rule, we need to predict the intermediate values $u(x_i, y_j, t^{n+1/2})$ and $u(x_i, y_j, t^{n+1})$. Once more, we use the smoothness of the approximations along the lines $(x_i, y_j) \times [t^n, t^{n+1}]$ to consider the Cauchy problem:

$$\begin{aligned}
&v'_{i,j}(\tau) = F(\tau, v_{i,j}(\tau)) = -f_x\,(v(x_i, y_j, t^n + \tau)) - g_y\,(v(x_i, y_j, t^n + \tau)), \\
&v_{i,j}(t_0) = u(x_i, y_j, t^n).
\end{aligned} \tag{2.7}$$

Similar to [2, 21], we use the Natural Continuous Extension (NCE) of Runge-Kutta (RK) methods [26] to solve the problem up to $\tau = \Delta t$. We use the second-order RK method given by the polynomials

$$b_1(\theta) = (b_1 - 1)\theta^2 + \theta, \tag{2.8}$$

$$b_2(\theta) = b_2\theta^2, \tag{2.9}$$

with the following set of coefficients:

$$b = \begin{pmatrix} 1/2 \\ 1/2 \end{pmatrix}, \quad a = \begin{pmatrix} 0 & 0 \\ 1 & 0 \end{pmatrix}. \tag{2.10}$$

To compute the predicted values of the quadrature formula $u(x_i, y_j, t^n + \beta_l \Delta t)$ efficiently, we rewrite the NCE-RK method as

$$\begin{aligned} u(x_i,\, y_j,\, t^n + \beta_l \Delta t) &= u_{ij}^n + \lambda \sum_{r=1}^{2} b_r(\beta_l) K_{ij}^r, \\ K_{ij}^r &= -f_x(Y_{ij}^r) - g_y(Y_{ij}^r), \\ Y_{ij}^r &= u_{ij}^n + \lambda \sum_{s=1}^{r-1} a_{rs} K_{ij}^s, \end{aligned} \tag{2.11}$$

where the coefficients a_{ij} are given in (2.10), and the numerical derivative f_x and g_y are discussed in the next section.

3 A Third-Order Non-Oscillatory Central Scheme

3.1 Reconstruction from Cell Averages

We first reconstruct the piecewise-polynomials $p_{i,j}^n(x,\, y)$ of (2.2). Following [16], we consider a polynomial of degree 2 associated with the cell $I_{i,j}$:

$$\begin{aligned} p_{i,j}^n(x,\, y) =& u_{i,j}^n + u_{x_{i,j}} \left(\frac{x - x_i}{h} \right) + u_{y_{i,j}} \left(\frac{y - y_j}{h} \right) \\ &+ \frac{1}{2h^2} \left(u_{xx_{i,j}} (x - x_i)^2 + 2u_{xy_{i,j}} (x - x_i)(y - y_j) + u_{yy_{i,j}} (y - y_j)^2 \right). \end{aligned} \tag{3.1}$$

We require that $p_{i,j}^n(x,\, y)$ obeys the conservation property:

$$\frac{1}{h^2} \int \int_{I_{ij}} p_{i,j}^n(x,\, y)\, dy\, dx = \overline{u}_{i,j}^n,$$

that is, $u_{i,j}^n$ must satisfy

$$u_{i,j}^n = \overline{u}_{i,j}^n - \frac{1}{24} \left(u_{xx_{i,j}} + u_{yy_{i,j}} \right). \tag{3.2}$$

We choose the numerical derivatives to be fully non-oscillatory as [5], compared to the CWENO reconstructions of [16] and [17]. In addition, they must yield third-order accuracy, that is,

$$\frac{1}{h} u_{x_{i,j}} = \frac{\partial}{\partial x} u(x = x_i,\, y = y_j,\, t^n) + \mathcal{O}(h^2), \tag{3.3}$$

$$\frac{1}{h} u_{y_{i,j}} = \frac{\partial}{\partial y} u(x = x_i,\, y = y_j,\, t^n) + \mathcal{O}(h^2), \tag{3.4}$$

$$\frac{1}{h^2} u_{xx_{i,j}} = \frac{\partial^2}{\partial x^2} u(x = x_i,\, y = y_j,\, t^n) + \mathcal{O}(h), \tag{3.5}$$

$$\frac{1}{h^2} u_{yy_{i,j}} = \frac{\partial^2}{\partial y^2} u(x = x_i,\, y = y_j,\, t^n) + \mathcal{O}(h), \tag{3.6}$$

$$\frac{1}{h^2} u_{xy_{i,j}} = \frac{\partial^2}{\partial x \partial y} u(x = x_i,\, y = y_j,\, t^n) + \mathcal{O}(h). \tag{3.7}$$

Using (3.1) and (3.2), the reconstruction of (2.4) gives

$$\begin{aligned}\overline{u}^n_{i+\frac{1}{2},j+\frac{1}{2}} =& \frac{1}{4}(\overline{u}^n_{i,j} + \overline{u}^n_{i+1,j} + \overline{u}^n_{i,j+1} + \overline{u}^n_{i+1,j+1}) \\ &+ \frac{1}{16}(u_{x_{i,j}} - u_{x_{i+1,j}} + u_{x_{i,j}} - u_{x_{i+1,j+1}}) \\ &+ \frac{1}{16}(u_{y_{i,j}} + u_{y_{i+1,j}} - u_{y_{i,j}} - u_{y_{i+1,j+1}}) \\ &+ \frac{1}{64}(u_{xy_{i,j}} - u_{xy_{i+1,j}} - u_{xy_{i,j}} + u_{xy_{i+1,j+1}}). \end{aligned} \tag{3.8}$$

In order to achieve third-order accuracy for (3.8), we use the UNO limiter to find the numerical derivatives (3.3), (3.4) and (3.7):

$$u_{x_{i,j}} = \mathrm{MM}\left\{\Delta\overline{u}_{i-\frac{1}{2},j} + \frac{1}{2}\mathrm{MM}\left\{\Delta^2\overline{u}_{i-1,j}, \Delta^2\overline{u}_{i,j}\right\}, \Delta\overline{u}_{i+\frac{1}{2},j} - \frac{1}{2}\mathrm{MM}\left\{\Delta^2\overline{u}_{i,j}, \Delta^2\overline{u}_{i+1,j}\right\}\right\}, \tag{3.9}$$

$$u_{y_{i,j}} = \mathrm{MM}\left\{\Delta\overline{u}_{i,j-\frac{1}{2}} + \frac{1}{2}\mathrm{MM}\left\{\Delta^2\overline{u}_{i,j-1}, \Delta^2\overline{u}_{i,j}\right\}, \Delta\overline{u}_{i,j+\frac{1}{2}} - \frac{1}{2}\mathrm{MM}\left\{\Delta^2\overline{u}_{i,j}, \Delta^2\overline{u}_{i,j+1}\right\}\right\}, \tag{3.10}$$

$$u_{xy_{i,j}} = \mathrm{MM}\left\{\Delta u_{y_{i-\frac{1}{2},j}} + \frac{1}{2}\mathrm{MM}\left\{\Delta^2 u_{y_{i-1,j}}, \Delta^2 u_{y_{i,j}}\right\}, \Delta u_{y_{i+\frac{1}{2},j}} - \frac{1}{2}\mathrm{MM}\left\{\Delta^2 u_{y_{i,j}}, \Delta^2 u_{y_{i+1,j}}\right\}\right\}. \tag{3.11}$$

One may alternatively find $u_{xy_{i,j}}$ of (3.11), by using the derivatives on the $y-$axis of $u_{x_{i,j}}$. Numerical experiments indicate that similar results are obtained.

The NT scheme [20] uses a second-order accurate limiter

$$v'_j = \mathrm{MM}\left(\Delta v_{j-\frac{1}{2}}, \Delta v_{j+\frac{1}{2}}\right), \tag{3.12}$$

which is non-oscillatory in the sense that

$$0 \le v'_j \cdot \mathrm{sign}(\Delta v_{j\pm\frac{1}{2}}) \le \mathrm{Const.} \cdot \left|\mathrm{MM}\left(\Delta v_{j-\frac{1}{2}}, \Delta v_{j+\frac{1}{2}}\right)\right|.$$

Here, $\Delta v_{j+\frac{1}{2}} = v_{j+1} - v_j$, and the MinMod limiter (MM) is defined by

$$\mathrm{MM}(x_1, x_2, \ldots) = \begin{cases} \min_p \{x_p\} & \text{if } x_p > 0 \ \forall p, \\ \max_p \{x_p\} & \text{if } x_p < 0 \ \forall p, \\ 0 & \text{otherwise.} \end{cases}$$

However, the accuracy of (3.12) drops at the non-sonic critical gridvalues v_j, where $\Delta v_{j-\frac{1}{2}} \cdot \Delta v_{j+\frac{1}{2}} < 0 \neq f'(v_j)$. NT scheme adapted the uniform non-oscillatory (UNO) limiter of Harten and Osher [4]

$$v'_j = \mathrm{MM}\left(\Delta v_{j-\frac{1}{2}} + \frac{1}{2}\mathrm{MM}\left(\Delta^2 v_{j-1}, \Delta^2 v_j\right), \Delta v_{j+\frac{1}{2}} - \frac{1}{2}\mathrm{MM}\left(\Delta^2 v_j, \Delta^2 v_{j+1}\right)\right), \tag{3.13}$$

where $\Delta^2 v_j = v_{j+1} - 2v_j + v_{j-1}$. The limiter (3.13) adds second-order differences to the MinMod limiter (3.12) to achieve high accuracy including at critical points.

3.2 Reconstruction from Point Values

We approximate the point-value $u^n_{i,j}$ of (3.2) from the cell averages $\overline{u}^n_{i,j}$, while simultaneously looking for high accuracy and avoiding oscillations. This is achieved by approximating the derivatives of (3.2) by

$$u_{xx_{i,j}} = \mathrm{MM}\left(\Delta^2\overline{u}^n_{i-1,j}, \Delta^2\overline{u}^n_{i,j}, \Delta^2\overline{u}^n_{i+1,j}\right), \tag{3.14}$$

$$u_{yy_{i,j}} = \mathrm{MM}\left(\Delta^2\overline{u}^n_{i,j-1}, \Delta^2\overline{u}^n_{i,j}, \Delta^2\overline{u}^n_{i,j+1}\right). \tag{3.15}$$

Following [21], we compute the MM limiter with three arguments as follows

$$\begin{aligned}\mathrm{MM}(x_1,\, x_2,\, x_3) =& \frac{1}{4}(\mathrm{sign}(x_1) + \mathrm{sign}(x_2) + \mathrm{sign}(x_3) + \mathrm{sign}(x_1\, x_2\, x_3)) \\ & \times \min(|x_1|, |x_2|, |x_3|).\end{aligned}$$

In order to compute the fluxes of (2.7), we must evaluate the function

$$F(u_{i,j}) = -f_x(u_{i,j}) - g_y(u_{i,j}), \tag{3.16}$$

where $u_{i,j}$ is found at the intermediate time intervals given by the NCE-RK method, notably for $u(x_i,\, y_j,\, t^{n+1/2})$ and $u(x_i,\, y_j,\, t^{n+1})$. The numerical derivatives of (3.16) must satisfy third-order accuracy, that is,

$$\frac{1}{h} f_x(u_{i,j}) = \frac{\partial}{\partial x} f(u(x = x_i,\, y = y_j,\, t^n)) + \mathcal{O}(h^2), \tag{3.17}$$

$$\frac{1}{h} g_y(u_{i,j}) = \frac{\partial}{\partial y} g(u(x = x_i,\, y = y_j,\, t^n)) + \mathcal{O}(h^2). \tag{3.18}$$

We approximate $f_x(u_{i,j})$ and $g_y(u_{i,j})$ in a similar way as in (3.9) and (3.10) by using the UNO limiter on differences of f and g to obtain the desired order of accuracy and still remain non-oscillatory. The derivatives of the fluxes are then given by

$$f_{x_{i,j}} = \mathrm{MM}\left\{\Delta f_{i-\frac{1}{2},j} + \frac{1}{2}\mathrm{MM}\left\{\Delta^2 f_{i-1,j},\, \Delta^2 f_{i,j}\right\},\, \Delta f_{i+\frac{1}{2},j} - \frac{1}{2}\mathrm{MM}\left\{\Delta^2 f_{i,j},\, \Delta^2 f_{i+1,j}\right\}\right\}, \tag{3.19}$$

$$g_{y_{i,j}} = \mathrm{MM}\left\{\Delta g_{i,j-\frac{1}{2}} + \frac{1}{2}\mathrm{MM}\left\{\Delta^2 g_{i,j-1},\, \Delta^2 g_{i,j}\right\},\, \Delta g_{i,j+\frac{1}{2}} - \frac{1}{2}\mathrm{MM}\left\{\Delta^2 g_{i,j},\, \Delta^2 g_{i,j+1}\right\}\right\}. \tag{3.20}$$

4 Numerical Experiments

Problem 1 We test the accuracy of the third-order scheme, which we call CNO3, on the 2D linear advection problem $u_t + u_x + u_y = 0$ with the initial condition $u(x,\, y,\, 0) = \sin^2(\pi x)\, \sin^2(\pi y)$ and periodic boundary conditions on the domain $[0,\, 1] \times [0,\, 1]$. In Table 1 we give the error and numerical order obtained on different grid sizes with $\lambda = 0.3$ at $T = 1$. We see that the scheme is converging to third-order accuracy, but it does not achieve the maximum order of accuracy due to the non-smooth limiters [24]. For comparison, we include the results obtained by the third-order central scheme with CWENO weights and constant weights of [16] for $\lambda = 0.425$. We see that those schemes give comparable convergence to our proposed scheme, but smaller magnitude of L_1 errors. Similar observations are made with the compact scheme of [15]. However, the fourth-order central scheme of [17] performs better as expected.

Problem 2 We consider the linear rotation problem of [17] where $u_t + f(u,x,y)_x + g(u,x,y)_y = 0$ on the square patch $[0,\, 1] \times [0,\, 1]$ with $N = 40$ in each direction and $\lambda = 0.3$. The initial condition and fluxes are respectively given by

$$u_0(x,\, y) = \begin{cases} 1, & |x - \frac{1}{2}| < \frac{1}{2} \text{ and } |y - \frac{1}{2}| < \frac{1}{2}, \\ 0, & \text{otherwise}, \end{cases}$$

and

$$f(u,x,y) = -\left(y - \frac{1}{2}\right)\frac{\pi u}{2}, \quad g(u,x,y) = \left(x - \frac{1}{2}\right)\frac{\pi u}{2}.$$

Figure 1 shows the solutions at $T = 0.5$ and $T = 1$ by the CNO3 scheme which are free from spurious oscillations.

Table 1. Accuracy by central schemes with $u(x, y, 0) = \sin^2(\pi x) \sin^2(\pi y)$.

N	CNO3			
	L_1 error	L_∞ error	L_1 error	L_∞ error
10	0.4988(-1)	–	0.1472	–
20	0.7054(-2)	2.822	0.2535(-1)	2.538
40	0.9287(-3)	2.925	0.3431(-2)	2.886
80	0.1220(-5)	2.928	0.4643(-3)	2.885
N	Constant weights		C-WENO weights	
	L_1 error	L_1 order	L_1 error	L_1 order
10	0.1570(-1)	–	0.8524(-1)	–
20	0.2667(-2)	2.558	0.2652(-1)	1.685
40	0.3434(-3)	2.944	0.4181(-2)	2.665
80	0.4386(-4)	2.982	0.4427(-4)	6.561

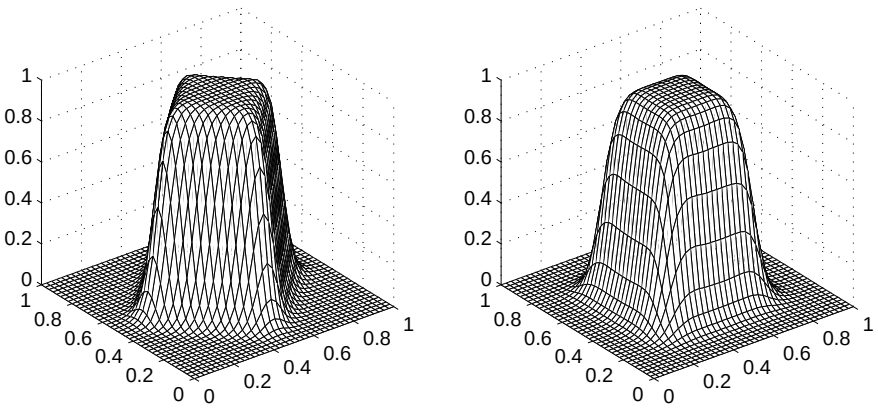

(a) $T = 0.5$ (b) $T = 1$

Figure 1. Solution of Problem 2 by CNO3, with $N = 40$ and $\lambda = 0.3$.

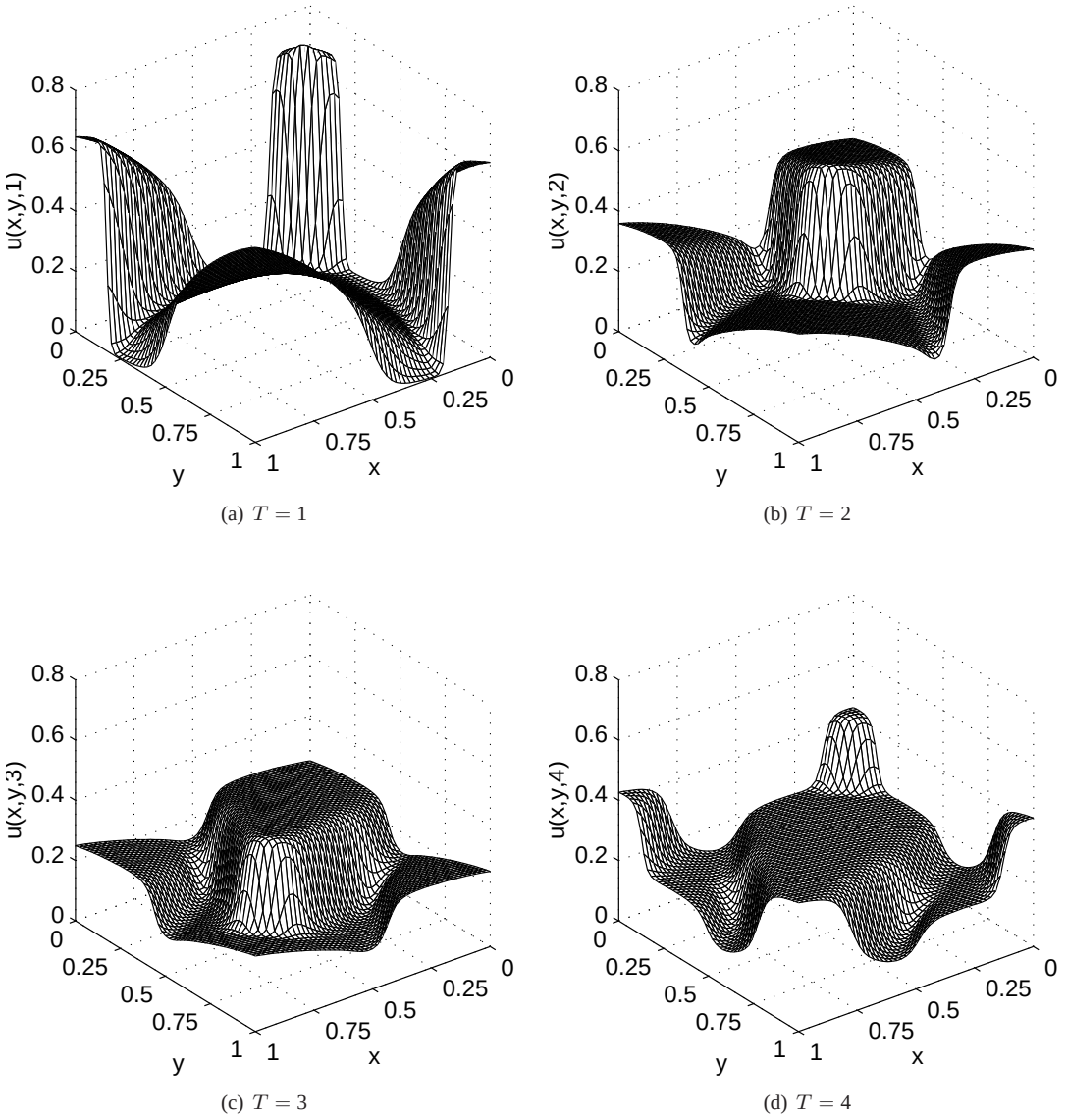

(a) $T = 1$ (b) $T = 2$

(c) $T = 3$ (d) $T = 4$

Figure 2. Solution of Burgers' equation by CNO3 with $\lambda = 0.3$ and $h = 0.02$.

Problem 3 We next solve the Burgers' equation $u_t + (\frac{1}{2}u^2)_x + (\frac{1}{2}u^2)_y = 0$ for the initial condition from [16], $u(x, y, 0) = \sin^2(\pi x)\, \sin^2(\pi y)$, on the domain $[0, 1] \times [0, 1]$ with periodic boundary conditions. In Figure 2, we display the results up to $T = 4$, on 50×50 grid with $\lambda = 0.3$. We observe that the solutions obtained by CNO3 are well resolved and non-oscillatory.

Problem 4 Finally, we test CNO3 on the Riemann problems for two-dimensional gas dynamics

$$U_t + F(U)_x + G(U)_y = 0,$$

where

$$U = \begin{pmatrix} \rho \\ \rho u \\ \rho v \\ E \end{pmatrix}, \; F(U) = \begin{pmatrix} \rho u \\ \rho u^2 + p \\ \rho uv \\ u(E+p) \end{pmatrix}, \; G(U) = \begin{pmatrix} \rho u \\ \rho uv \\ \rho v^2 + p \\ v(E+p) \end{pmatrix},$$

and $E = \frac{p}{(\gamma-1)} + \frac{1}{2}\rho(u^2+v^2)$. Here ρ is the density, u and v are the velocity components, E is the total energy and p is the pressure. $\gamma = 1.4$ is the ratio of specific heats.

Nineteen configurations were identified for those problems [22, 23, 13, 12], where the initial condition on $[0,1]\times[0,1]$ is given by

$$(p,\,\rho,\,u,\,v)(x,\,y,\,0) = \begin{cases} (p_1,\,\rho_1,\,u_1,\,v_1), & \text{if } x > 0.5,\ y > 0.5,\\ (p_2,\,\rho_2,\,u_2,\,v_2), & \text{if } x < 0.5,\ y > 0.5,\\ (p_3,\,\rho_3,\,u_3,\,v_3), & \text{if } x < 0.5,\ y < 0.5,\\ (p_4,\,\rho_4,\,u_4,\,v_4), & \text{if } x > 0.5,\ y < 0.5. \end{cases}$$

The different quadrants are initially separated by either rarefaction, shock or contact wave. We tested all the different configurations using componentwise extension with $\lambda = 0.3$ and 200×200 grid but due to space constraints we show only a few results in Figure 3. We observe that CNO3 recovers the major features on the density profiles in most test cases, but is somewhat smeared near discontinuities.

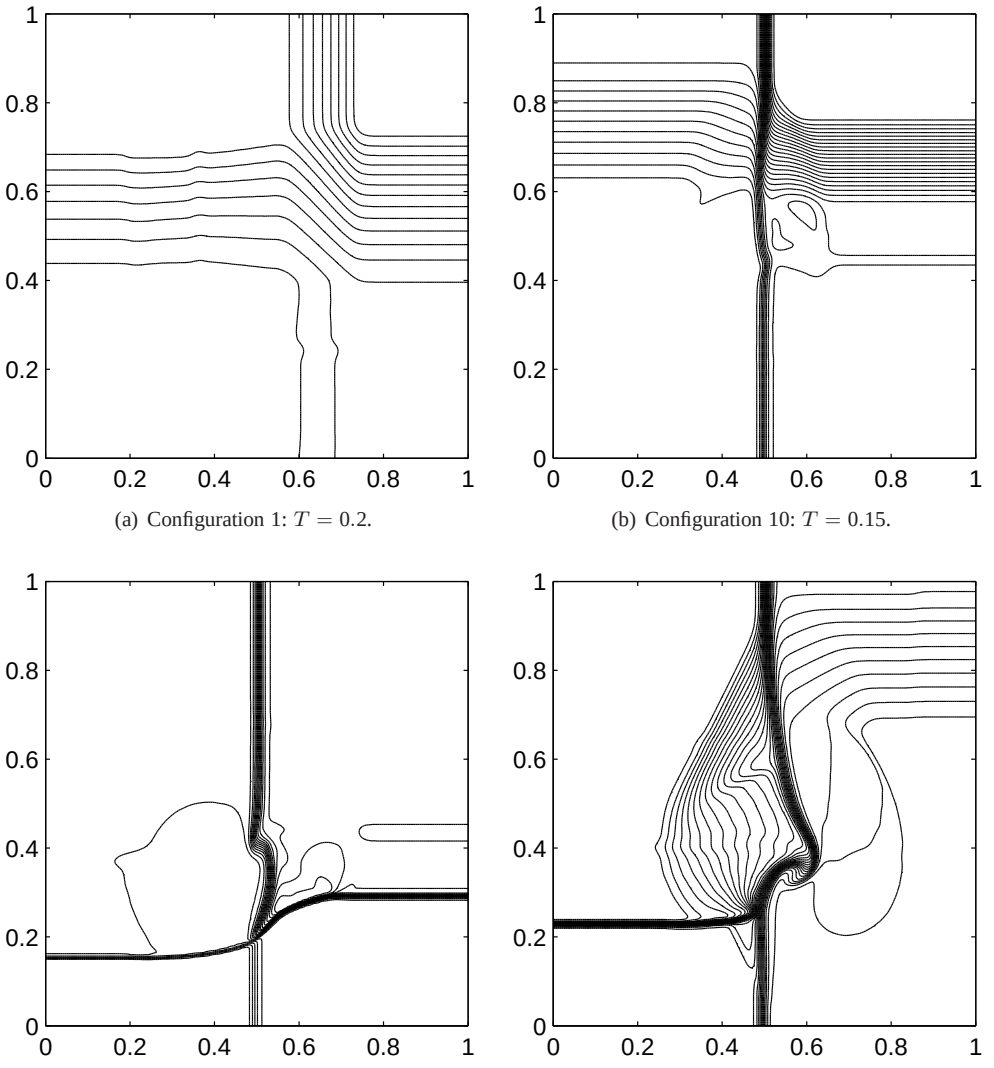

(a) Configuration 1: $T = 0.2$.

(b) Configuration 10: $T = 0.15$.

(c) Configuration 14: $T = 0.1$.

(d) Configuration 19: $T = 0.3$.

Figure 3. Approximation of some two-dimensional gas dynamics problems by CNO3

5 Conclusion

In this work, we have introduced a genuinely multidimensional third-order non-oscillatory central scheme. A piecewise quadratic polynomial is used for the reconstruction, which uses high-order accurate approximation for the spatial derivatives to avoid spurious oscillations. The scheme was tested on different problems and we observed that it captured the right profile of the solutions. However, the scheme is damped and discontinuities were smeared due to the non-linear limiter. Alternatively, a sharper non-oscillatory multi-dimensional reconstruction may be used, but this will necessitate additional numerical derivatives. The proposed scheme can also be extended to solve Hamilton-Jacobi equations [19] and MHD equations [1].

References

[1] J. Balbas, E. Tadmor, and C.-C. Wu. Non-oscillatory central schemes for one-and two-dimensional MHD equations: I. *J. Comput. Phys.*, 201(1):261–285, 2004.

[2] F. Bianco, G. Puppo, and G. Russo. High-order central schemes for hyperbolic systems of conservation laws. *SIAM J. Sci. Comput.*, 21(1):294–322, 1999.

[3] M. Geiben, D. Kröner, and M. Rokyta. A Lax-Wendroff type theorem for cell-centered, finite volume schemes in 2-D. *preprint*, 278(SFB256), 1991.

[4] A. Harten and S. Osher. Uniformly high-order accurate nonoscillatory schemes, I. *SIAM J. Numer. Anal.*, 24(2):279–309, 1987.

[5] G. S. Jiang and E. Tadmor. Nonoscillatory central schemes for multidimensional hyperbolic conservation laws. *SIAM J. Sci. Comput.*, 19(6):1892–1917, 1998.

[6] T. Katsaounis and D. Levy. A modified structured central scheme for 2D hyperbolic conservation laws. *Applied mathematics letters*, 12(6):89–96, 1999.

[7] D. Kröner. *Numerical Schemes for Conservation Laws*. Wiley Teubner, Chichester, 1997.

[8] A. Kurganov and D. Levy. A third-order semidiscrete central scheme for conservation laws and convection-diffusion equations. *SIAM J. Sci. Comput.*, 22(4):1461–1488, 2000.

[9] A. Kurganov, S. Noelle, and G. Petrova. Semidiscrete central-upwind schemes for hyperbolic conservation laws and hamilton-jacobi equations. *SIAM J. Sci. Comput.*, 23(3):707–740, 2001.

[10] A. Kurganov and G. Petrova. A third-order semi-discrete genuinely multidimensional central scheme for hyperbolic conservation laws and related problems. *Numer. Math.*, 88:683–729, 2001.

[11] A. Kurganov and E. Tadmor. New high-resolution central schemes for nonlinear conservation laws and convection-diffusion equations. *J. Comput. Phys.*, 160:241–282, 2000.

[12] A. Kurganov and E. Tadmor. Solution of two-dimensional Riemann problems for gas dynamics without Riemann problem solvers. *Numer. Meth. Partial Differ. Eq.*, 18:584–608, 2002.

[13] P. D. Lax and X.-D. Liu. Solution of two-dimensional Riemann problems of gas dynamics by positive schemes. *SIAM J. Sci. Comput.*, 19:319–340, 1998.

[14] R. J. LeVeque. *Finite Volume Methods for Hyperbolic Problems*. Cambridge University Press, Cambridge, UK, 2002.

[15] D. Levy, G. Puppo, and G. Russo. Compact central WENO schemes for multidimensional conservation laws. *SIAM J. Sci. Comput.*, 22(2):656–672, 2000.

[16] D. Levy, G. Puppo, and G. Russo. A third order central WENO scheme for 2D conservation laws. *Appl. Numer. Math.*, 33:415–421, 2000.

[17] D. Levy, G. Puppo, and G. Russo. A fourth-order central WENO scheme for multidimensional hyperbolic systems of conservation laws. *SIAM J. Sci. Comput.*, 24(2):480–456, 2002.

[18] G. Li, V. Caleffi, and J. Gao. High-order well-balanced central WENO scheme for pre-balanced shallow water equations. *Computers and Fluids*, 99:182–189, 2014.

[19] C.-T. Lin and E. Tadmor. High-resolution nonoscillatory central schemes for hamilton–jacobi equations. *SIAM J. Sci. Comput.*, 21(6):2163–2186, 2000.

[20] H. Nessyahu and E. Tadmor. Non-oscillatory central differencing for hyperbolic conservation laws. *J. Comput. Phys.*, 87(2):408–463, 1990.

[21] A. A. I. Peer, A. Gopaul, M. Z. Dauhoo, and M. Bhuruth. A new fourth-order non-oscillatory central scheme for hyperbolic conservation laws. *Appl. Numer. Math.*, 58:674–688, 2008.

[22] C. W. Schulz-Rinne. Classification of the Riemann problem for two-dimensional gas dynamics. *SIAM J. Math. Anal.*, 24:77–88, 1993.

[23] C. W. Schulz-Rinne, J. P. Collins, and H. M. Glaz. Numerical solution of the Riemann problem for two-dimensional gas dynamics. *SIAM J. Sci. Comput.*, 14:1394–1414, 1993.

[24] S. Serna and A. Marquina. Power ENO methods: a fifth-order accurate Weighted Power ENO method. *J. Comput. Phys.*, 194:632–658, 2004.

[25] E. F. Toro. *Riemann Solvers and Numerical Methods for Fluid Dynamics: A Practical Introduction*. Springer-Verlag, Berlin, 1999.

[26] M. Zennaro. Natural continuous extensions of Runge-Kutta methods. *Math. Comput.*, 46:119–133, 1986.

Author information

A. A. I. Peer, A. A. E. F. Saib, M. S. Sunhaloo, Department of Applied Mathematical Sciences, University of Technology, Mauritius, La Tour Koenig, Pointe-aux-Sables 11134, Mauritius.
E-mail: apeer@umail.utm.ac.mu, asaib@umail.utm.ac.mu, ssunhaloo@umail.utm.ac.mu

M. Bhuruth, Department of Mathematics, University of Mauritius, Reduit 80837, Mauritius.
E-mail: mbhuruth@uom.ac.mu

Received: May 10, 2015.

Accepted: July 11, 2015